

Ocean acidification increases iodine accumulation in kelp-based coastal food webs

Xu, Dong; Brennan, Georgina; Xu, Le; Zhang, Xiao W.; Fan, Xiao; Han, Wen T.; Mock, Thomas; McMinn, Andrew; Hutchins, David A.; Ye, Naihao

Global Change Biology

DOI:
[10.1111/gcb.14467](https://doi.org/10.1111/gcb.14467)

Published: 01/02/2019

Peer reviewed version

[Cyswllt i'r cyhoeddiad / Link to publication](#)

Dyfyniad o'r fersiwn a gyhoeddwyd / Citation for published version (APA):

Xu, D., Brennan, G., Xu, L., Zhang, X. W., Fan, X., Han, W. T., Mock, T., McMinn, A., Hutchins, D. A., & Ye, N. (2019). Ocean acidification increases iodine accumulation in kelp-based coastal food webs: Ocean acidification increases iodine in kelp. *Global Change Biology*, 25(2), 629-639. <https://doi.org/10.1111/gcb.14467>

Hawliau Cyffredinol / General rights

Copyright and moral rights for the publications made accessible in the public portal are retained by the authors and/or other copyright owners and it is a condition of accessing publications that users recognise and abide by the legal requirements associated with these rights.

- Users may download and print one copy of any publication from the public portal for the purpose of private study or research.
- You may not further distribute the material or use it for any profit-making activity or commercial gain
- You may freely distribute the URL identifying the publication in the public portal ?

Take down policy

If you believe that this document breaches copyright please contact us providing details, and we will remove access to the work immediately and investigate your claim.

1 **Ocean acidification increases iodine accumulation in kelp-based**
2 **coastal food webs**

3 **Running head:** Ocean acidification increases iodine in kelp

4 Dong Xu^{1,2,#}, Georgina Brennan^{3,#}, Le Xu¹, Xiao W. Zhang¹, Xiao Fan¹, Wen T. Han¹,
5 Thomas Mock⁴, Andrew McMinn^{5,6}, David A. Hutchins⁷, Naihao Ye^{1,2,*}

6 ¹Yellow Sea Fisheries Research Institute, Chinese Academy of Fishery Sciences,
7 Qingdao, China

8 ²Function Laboratory for Marine Fisheries Science and Food Production Processes,
9 Qingdao National Laboratory for Marine Science and Technology, Qingdao, China

10 ³Molecular Ecology and Fisheries Genetics Laboratory, School of Biological
11 Sciences, Bangor University, Bangor LL57 2UW, UK

12 ⁴School of Environmental Sciences, University of East Anglia, Norwich Research
13 Park, Norwich, United Kingdom

14 ⁵Institute for Marine and Antarctic Studies, University of Tasmania, Hobart,
15 Tasmania, Australia

16 ⁶Fisheries College, Ocean University of China, Qingdao, China

17 ⁷Department of Biological Sciences, University of Southern California, Los Angeles,
18 CA, USA

19 [#]These authors contributed equally to this work.

20 **Correspondence:** Naihao Ye, tel. 86-532-85830360, fax 86-532-85830360, e-mail:
21 yenh@ysfri.ac.cn.

22 **Keywords:** Ocean acidification, iodine metabolism, *Saccharina japonica*, kelp,

23 vanadium-dependent haloperoxidase, thyroid hormone

24 **Paper type:** Primary Research Article

25 Accepted for Publication in Global Change Biology (19th Sept 2018).

26

27

28

29

30

31

32

33

34

35

36

37

38

39

40

41

42

43

44

45

46 **ABSTRACT**

47 Kelp are main iodine accumulators in the ocean, and their growth and photosynthesis
48 are likely to benefit from elevated seawater CO₂ levels due to ocean acidification.
49 However, there are currently no data on the effects of ocean acidification on iodine
50 metabolism in kelp. As key primary producers in coastal ecosystems worldwide, any
51 change in their iodine metabolism caused by climate change will potentially have
52 important consequences for global geochemical cycles of iodine, including iodine
53 levels of coastal food webs that underpin the nutrition of billions of humans around the
54 world. Here, we found that elevated *p*CO₂ enhanced growth and increased iodine
55 accumulation not only in the model kelp *Saccharina japonica* using both short-term
56 laboratory experiment and long-term *in situ* mesocosms, but also in several other edible
57 and ecologically significant seaweeds using long-term *in situ* mesocosms.
58 Transcriptomic and proteomic analysis of *Saccharina japonica* revealed that most
59 vanadium-dependent haloperoxidase genes involved in iodine efflux during oxidative
60 stress are down-regulated under increasing *p*CO₂, suggesting that ocean acidification
61 alleviates oxidative stress in kelp, which might contribute to their enhanced growth.
62 When consumed by abalone (*Haliotis discus*), elevated iodine concentrations in *S.*
63 *japonica* caused increased iodine accumulation in abalone, accompanied by reduced
64 synthesis of thyroid hormones. Thus, our results suggest that kelp will benefit from
65 ocean acidification by a reduction in environmental stress however, iodine levels in
66 kelp-based coastal food webs will increase, with potential impacts on biogeochemical

cycles of iodine in coastal ecosystems.

INTRODUCTION

Anthropogenic emissions of CO₂, associated ocean acidification (OA) and global warming, are increasing at rates unprecedented in the geological record (Sunday et al., 2017; Thomsen et al., 2017). These changes are expected to directly affect primary producers by changing growth rates, photosynthesis and metabolism, and indirectly by reducing biodiversity and altering ecosystem structure (Enochs et al., 2015; Martínez-Botí et al., 2015; Myers et al., 2017; Ullah, Nagelkerken, Goldenberg, & Fordham, 2018). Furthermore, OA is predicted to cause an increase in the accumulation of toxic phenolic compounds across multiple trophic levels, from phytoplankton to zooplankton (Jin et al., 2015). Higher temperatures are also expected to increase the concentrations of nutrients such as nitrogen (N), potassium (K), and magnesium (Mg) stored in living biomass (Zhang et al., 2018) and impact the global biotic metabolic rates (Dillon, Wang, & Huey, 2010). Metabolic rate changes and nutrient variation under climate change will affect human health through consumption of these organisms (Jin et al., 2015; McKibben et al., 2017; Zhu et al., 2018) and potentially impact food security (Bloom, Burger, Asensio, & Cousins, 2010; Loladze, 2002; Myers et al., 2017; Phalkey, Aranda-Jan, Marx, Höfle, & Sauerborn, 2015). However, climate impacts on the nutrient composition of primary producers (such as, seaweeds) in coastal ecosystem has, to date, been little explored.

Seaweeds, including, brown, red, and green algae are a rich source of iodine (Küpper, 2015; Küpper et al., 2008; Nitschke & Stengel, 2015; Ye et al., 2015) and are widely harvested for food and exploited for commercial alginate and iodine. Iodine is an essential nutrient required for the synthesis of thyroid hormones (THs), triiodothyronine (T3) and thyroxine (T4) (Berg et al., 2017). Iodine deficiency in humans can result in unexpected health problems such as hypothyroidism and goiter, whereas high iodine intake from seaweeds can lead to hyperthyroidism, a reversible condition which can cause symptoms such as nontoxic or diffuse nodular goiter, latent Graves' disease and long standing iodine deficiency (Leung & Braverman, 2014). Natural consumers of seaweeds such as fish and shellfish are also a rich dietary source of iodine for humans (Nitschke & Stengel, 2015). It is therefore essential to understand how the iodine content of seafood will change under global climate change. This information can for instance be used by the World Health Organization (WHO) to provide recommendations on appropriate levels of seaweeds consumption to maintain a sufficient daily iodine intake (Fig. 1).

With respect to iodine, kelp (order Laminariales) are particularly important as they are not only being the greatest iodine accumulators among living organisms, but also playing an important role in the global biogeochemical cycle of iodine (Küpper, 2015; Küpper et al., 2008). In *Laminaria* tissue, iodine is mostly stored as iodide on the thallus surface and in the apoplast. Iodide efflux occurs under oxidative stress and iodide in the peripheral tissues acts as an inorganic antioxidant to detoxify both aqueous oxidants

and ozone, stimulating the release of molecular iodine and volatile iodinated compounds to the atmosphere (Cosse et al., 2009; Küpper & Kroneck, 2014). Oxidative burst and associated iodine metabolism also play a direct defensive role in both controlling the growth of potentially pathogenic bacteria living at the thallus surface and scavenging a variety of reactive oxygen species (ROS) (Küpper et al., 2008; Küpper, Müller, Peters, Kloareg, & Potin, 2002; Strittmatter et al., 2016). During oxidative burst, algal cells rapidly release large amounts of activated oxygen species (AOS), such as superoxide (O_2^-), hydrogen peroxide (H_2O_2) or hydroxyl radicals (OH^-). This release is elicited by exposure to oligomeric degradation products of alginate and possibly other molecular signals. It has been suggested that the mechanism of iodine antioxidation is linked to the production of vanadium-dependent haloperoxidases (vHPOs), which comprises seventeen vanadium-dependent bromoperoxidases (vBPOs) and fifty-nine iodoperoxidases (vIPOs) in the *S. japonica* genome (Butler & Carter-Franklin, 2004; Cosse et al., 2009; Ye et al., 2015) (Fig. 1).

Despite widespread interest in the biological response of kelp to climate change, there is currently no information on the *in situ* molecular response associated with iodine metabolism. Here, three ecologically and socio-economically important kelp species (*S. japonica*, *U. pinnatifida*, and *M. pyrifera*), as well as another four coastal seaweeds (*Ulva pertusa* and *Ulva intestinalis* in Chlorophyta; *Gracilaria lemaneiformis* and *Gracilaria chouae* in Rhodophyta) were used to study the effect of increasing pCO_2 on iodine accumulation of seaweeds using both short-term laboratory experiments and one

long-term, *in situ* experiment. In a feeding experiment, the transfer of iodine between *S. japonica* and its consumer *Haliotis discus* was investigated. We used these experiments to explore: (i) the effect of elevated $p\text{CO}_2$ on iodine accumulation in kelp-based coastal food webs; (ii) whether short-term laboratory experiments can be compared with *in situ* ocean mesocosms; (iii) the molecular mechanism involved in iodine metabolism at the transcriptional and protein level in response to elevated $p\text{CO}_2$. Together, the research presented here will be used to assess the global biogeochemical cycle of iodine under future climate change and provide information for making recommendations on appropriate levels of seaweeds consumption to reach adequate daily iodine intake.

MATERIALS AND METHODS

Algal material and culture conditions

For the laboratory experiments, young sporophytes of *S. japonica* were collected from semi-enclosed Sungo Bay, located on the northwestern coast of the Yellow Sea, China ($37^{\circ}01' - 37^{\circ}09' \text{ N}$, $122^{\circ}24' - 122^{\circ}35' \text{ E}$) in December 2016, when the mean seawater temperature was 10.3°C . Similar sized algal samples (average length is 10 cm) were transported back to the laboratory within three hours, in a tank of cold seawater. In the laboratory, the intact samples were washed with sterile seawater until they were free from visible epiphytes and then pre-cultured in aquaria supplemented with f/2 medium (Guillard, 1975) at $10 \pm 1^{\circ}\text{C}$ with vigorous air bubbling for 2 days before the start of the experiment. The lighting conditions were set at $100 \mu\text{mol photons m}^{-2} \text{ s}^{-1}$ supplied

by white fluorescent lamps, with a photoperiod of 12 h light and 12 h darkness.

Effect of increasing $p\text{CO}_2$ and temperature on iodine accumulation

To study the individual effect of temperature on iodine accumulation in *S. japonica* sporophytes, a gradient of five temperatures (5°C, 10°C, 15°C, 20°C, and 23°C) was established, mimicking the annual variation of temperature during the growth period. To examine the combined effect of increasing $p\text{CO}_2$ and temperature, three temperatures (10°C, 15°C, 20°C) and five $p\text{CO}_2$ levels (400 μatm , 700 μatm , 1,000 μatm , 1,500 μatm , and 2,000 μatm), were selected (Table S1). These $p\text{CO}_2$ levels were chosen as they reflect current and future $p\text{CO}_2$ levels up to the year 2,300 under IPCC (Intergovernmental Panel on Climate Change) scenario RCP 8.5. The experiment was conducted in flasks using three biological replicates per treatment. Before experiments, algal samples were pre-cultured in seawater under various $p\text{CO}_2$ and temperature conditions for 96 hours. Pre-cultured algae were then inoculated into 500-mL Erlenmeyer flasks containing 400 mL of adjusted f/2 seawater medium and supplemented with 20 $\mu\text{mol L}^{-1}$ KI (half saturation concentration derived from iodine uptake kinetics, in Fig. S1) for 24 h. At the end of the experiment, algal samples in each treatment were collected and rinsed for iodine determination within 24 h. Individual flasks were cultured inside a CO_2 chamber (HP1000G-D, China), programmed to supply 400 μatm , 700 μatm , 1,000 μatm , 1,500 μatm , or 2,000 μatm $p\text{CO}_2$ by bubbling at each designated temperature for 24 h. The pH and temperature were measured at the beginning and end of the experiment with a pH meter (Orion ROSS, Fisher Scientific

Instruments). To determine total alkalinity (TA) at each treatment, 20 ml of culture medium was filtered with GF/F membrane and measured using an 848 Titrino plus automatic titrator (Metrohm, Riverview, FL, USA). Chemical carbonate system parameters were calculated using the CO2SYS Package in MS Excel (Pierrot, Lewis, & Wallace, 2006) based on pH, temperature, salinity, and TA (Table S1).

Potential antioxidant property of iodide in *S. japonica*

To determine the potential antioxidant properties of iodide in *S. japonica*, oligoguluronate elicitor (GG, Shanghai Zzbio Co, Ltd, China) was used as exogenous defense elicitors to induce oxidative stress and iodine efflux from algal tissue into the culture medium (referred to previous study of (Küpper, Kloareg, Guern, & Potin, 2001). Algal samples were inoculated into 150-mL Erlenmeyer flasks containing 100 mL sterile seawater without (set as control) or with exogenous oligoguluronate elicitors at a final concentration of 100 µg ml⁻¹ (GG, set as treatment). Three elicitation experiments were conducted at 10°C and 100 µmol photons m⁻² s⁻¹. To understand the effect of GG on iodine efflux over time, three seawater samples were randomly taken from the untreated control and GG treatments at four time intervals (0 h, 1 h, 3 h, and 5 h). To understand the effect of elevated *p*CO₂ in the presence of GG, iodine efflux was measured after 3 hours under five *p*CO₂ conditions (400 µatm, 700 µatm, 1,000 µatm, 1,500 µatm, or 2,000 µatm, bubbled at 10°C for 24 h). To investigate the prolonged effect of ocean acidification on iodine efflux, the short-term vs long-term response of iodine efflux in *S. japonica* under ocean acidification conditions was compared. Under

short-term-ambient-carbon (SAC) and short-term-elevated-carbon (SEC) treatments, algae were pre-cultured at CO₂ concentrations of 400 µatm and 1,000 µatm respectively, for 7 days. Under long-term-ambient-carbon (LAC) or long-term-elevated-carbon (LEC) treatments, algae were pre-cultured under the same pCO₂ levels for 30 days. Following pre-culturing, iodine efflux under ambient (400 µatm) or elevated (1,000 µatm) pCO₂ was measured after 3 hours.

***In situ* mesocosm experiments**

Three kelp species, *S. japonica*, *U. pinnatifida*, and *M. pyrifera*, as well as other coastal seaweeds (*Ulva pertusa* and *Ulva intestinalis* in Chlorophyta; *Gracilaria lemaneiformis* and *Gracilaria chouae* in Rhodophyta) were collected off the coastline of Sungo Bay for the mesocosm experiment (Fig. S2). With the exception of *M. pyrifera*, these algae are widely consumed by humans. *M. pyrifera* was selected as it is a preferred food source of marine invertebrates, such as sea urchins and abalone, which are harvested by the local fishing industry. The mesocosms were designed following (Xu et al., 2017). Six net cages (three per treatment) were used, applying two pCO₂ levels, ambient pCO₂ (400 µatm, bubbled with air) and elevated pCO₂ (1,000 µatm, bubbled with air/CO₂ premixed gas using a CO₂ Enrichlor, CE-100B; Wuhan Ruihua Instrument & Equipment Ltd) (Fig. S3). One hundred and twenty individuals of each algal species of similar size were grown in each cage for approximately five months, from December 2016 to May 2017. During this period, six individuals of each algal species from each net cage (n=6) were randomly collected for iodine determination, and 10 individuals

(n=10) from each net cage were selected and weighed to monitor growth. To determine the effect of kelp size on iodine accumulation during the culture period, kelp which were pre-acclimated under ambient or elevated $p\text{CO}_2$ for 48 hours in the sea were sampled at different time points: 0 day, 30 days, 60 days, and 90 days for *S. japonica*, 0 day, 30 days, and 60 days for *U. pinnatifida*, and 0 day, 20 days, and 40 days for *M. pyrifera*. Seawater carbonate chemistry in the ambient (400 μatm) or elevated (1,000 μatm) $p\text{CO}_2$ culture environments were monitored every two days and the carbonate chemistry was calculated using the CO2SYS Package in MS Excel based on pH, temperature, salinity, and TA (Fig. S4) (for further details of the mesocosm design, see methods in supporting information).

To assess the effects of consumption of *S. japonica* by abalone, sporophytes were grown at either ambient (400 μatm) or elevated (1,000 μatm) $p\text{CO}_2$. Five feeding experiments were conducted *in situ*: 1) abalones were fed with ambient $p\text{CO}_2$ -cultured *S. japonica* and were also cultured in an ambient $p\text{CO}_2$ -cage; 2) abalones were fed with ambient $p\text{CO}_2$ -cultured *S. japonica* and were cultured in an elevated $p\text{CO}_2$ -cage; 3) abalones were fed with elevated $p\text{CO}_2$ -cultured *S. japonica* and were also cultured in an elevated $p\text{CO}_2$ -cage; 4) abalones were fed with elevated $p\text{CO}_2$ -cultured *S. japonica* and were cultured in an ambient $p\text{CO}_2$ -cage; 5) abalones were fed with ambient $p\text{CO}_2$ -cultured *S. japonica* and were cultured in the sea with no cage; 6) abalones were fed with elevated $p\text{CO}_2$ -cultured *S. japonica* and were cultured in the sea with no cage. The experiments, with six replicates ($n = 6$), were conducted independently for 30 days, starting on April

10th 2017. The experimental abalones were fed with fresh algal tissue at intervals of 3 days and collected for iodine determination at intervals of 10 days. At the end of the experiments, the abalones were cleaned with sterile seawater and the tissue was removed quickly and entirely from the shell, weighed and frozen in liquid nitrogen, and stored at -80 °C for total iodine and thyroid hormones (THs) determination (see methods in supporting information).

Transcriptomic and proteomic analysis of iodine metabolism in *S. japonica*

To explore the effect of ocean acidification on the iodine metabolism on the *S. japonica* transcriptome, on day 90 of the mesocosm experiment, *S. japonica* sporophytes were randomly selected, cleaned with sterile seawater, frozen in liquid nitrogen and stored at -80 °C for subsequent transcriptomic (with three biological replicates for each $p\text{CO}_2$) and proteomic (with two biological replicates for each $p\text{CO}_2$) analysis (see methods in supporting information).

Statistical analysis

Statistical models were carried out with R software (R Core Development Team, 2014) and model selection was based by Akaike Information Criterion (AIC). The effect of temperature and the combined effect of increasing $p\text{CO}_2$ and temperature on iodine accumulation were analyzed using a mixed effects model using the lmer function within the package lme4 and lmerTest. When modelling the effect of temperature alone, temperature was used as a fixed factor, when modelling the combined effect of

temperature and $p\text{CO}_2$, both temperature and $p\text{CO}_2$ were used as fixed factors (the interaction between temperature and $p\text{CO}_2$ was dropped from the model based on AIC). The effect of measurement type, either iodide or total iodine accumulation, were used as random factors in both models.

Using the `lm` function within R, three liner models were used to compare changes in iodine efflux in *S. japonica* treated with oligoguluronates (GG) or untreated (control). To test for the effect of time (hours) on iodine efflux, time, treatment (GG or control), and the interaction between time and treatment were included in a linear model. The effect of increasing $p\text{CO}_2$ (400 to 2000 μatm), treatment (GG or control), and the interaction between $p\text{CO}_2$ and treatment were included in a second linear model. The effect of ambient and elevated $p\text{CO}_2$, treatment (GG or control), time (days), the interaction between $p\text{CO}_2$ and time, and the interaction between treatment and $p\text{CO}_2$ were included in a third linear model.

In order to compare the responses of the three species of seaweeds used in the mesocosm experiment (*S. japonica*, *M. pyrifera* and *U. pinnatifida*), the relative change in iodine accumulation and weight (g) over time were calculated, relative to the responses at time point zero, under control conditions (400 μatm). To test for the effect of $p\text{CO}_2$ (ambient or elevated), over time (days), on relative changes in iodine accumulation, the effect of $p\text{CO}_2$, time, species and the interactions between time and species were included in a linear model. To test for the effect of $p\text{CO}_2$, over time, on

the relative weight of the seaweeds, the effect of $p\text{CO}_2$, time, species and the interaction between $p\text{CO}_2$, time and species were included in a linear model.

Three linear models were used to test the effect of diet and $p\text{CO}_2$ on 1) iodine enrichment 2) T3 concentration and 3) T4 concentration in the abalone (*H. discus*). For iodine enrichment, the effect of diet, time, $p\text{CO}_2$, the interaction between diet, time and $p\text{CO}_2$, and environment (caged or non-caged) were included in the model. For both T3 and T4 hormones, the effect diet, $p\text{CO}_2$, environment (caged or non-caged) and the interaction between environment and diet were included in the model. Data collected for iodine enrichment and T3 concentration best fit a lognormal distribution and for this reason a generalized linear model which takes into consideration a lognormal distribution was carried out, using the glm function in the stats package.

RESULTS

Effect of increasing $p\text{CO}_2$ and temperature on iodine accumulation of *S. japonica* in laboratory

Elevated $p\text{CO}_2$ caused changes in iodine accumulation in *S. japonica* when both the $p\text{CO}_2$ and temperature were altered at the same time (Fig. 2a; $F_{1,86} = 14.515$, $P = 0.0003$), with no significant effect of temperature on iodine accumulation (Fig. 2a; $F_{1,86} = 1.507$, $P = 0.223$). As $p\text{CO}_2$ increased from 400 μatm to 1,000 μatm at the control temperature (10 °C), both iodide and total iodine increased and reached the highest observed iodine accumulation at 1,000 μatm . As $p\text{CO}_2$ increased to 1,500 μatm , iodide and total iodine

accumulation decreased and leveled off as $p\text{CO}_2$ increased to 2,000 μatm . When temperature was altered in isolation, there was a significant effect on iodide and total iodine accumulation in *S. japonica* (Fig. 2b; $F_{1,27} = 19.47$, $P = 0.0002$). As temperature increased, from 5 °C to 15 °C under the control $p\text{CO}_2$ concentration (400 μatm), iodide and total iodine accumulation increased by 64% and 58%, respectively (Fig. 2b). At 20 °C and 23 °C, iodine accumulation decreased slightly but it was not significantly different from the maximum iodine accumulation observed at 15 °C. However, there were no significant effects of increasing $p\text{CO}_2$ or temperature (isolation or combination) on iodine solubility and availability in seawater medium (Fig. S5).

Potential antioxidant properties of iodide in *S. japonica* in laboratory

Under oxidative stress, induced by the addition of oligoguluronates (GG), iodine efflux in *S. japonica* was 61% greater than the untreated control group, after 5 hours (Fig. 3a; $F_{1,225} = 22.428$, $P = 0.0001$). Iodine efflux in *S. japonica* treated with GG increased over three hours and then decreased slightly after five hours, with little change in the untreated control group over time (Fig. 3a; *effect of time on the iodine efflux*, $F_{1,47} = 4.685$, $P = 0.0427$) and is supported by a significant interaction between the treatment (GG and control) and time (Fig. 3a; $F_{1,20} = 4.562$, $P = 0.0452$).

Iodine efflux in *S. japonica* increased with increasing $p\text{CO}_2$ until 1500 μatm and decreased again at 2000 μatm (Fig. 3b; $F_{1,10} = 2.95$, $P = 0.098$). Iodine efflux was 51% - 72% higher in *S. japonica* treated with GG than the untreated group, depending on the

$p\text{CO}_2$ levels (Fig. 3b; $F_{1,475} = 148.375$, $P < 0.0001$), and this is supported by a significant interaction between the $p\text{CO}_2$ conditions and treatment (GG and untreated) (Fig. 3b; $F_{1,17} = 5.173$, $P = 0.031$).

Long-term exposure to elevated $p\text{CO}_2$ (LEC) intensified iodine efflux from *S. japonica*. Iodine efflux from *S. japonica* treated with GG was 29% higher after 30 days exposure to elevated $p\text{CO}_2$, compared with 7 days of exposure to elevated $p\text{CO}_2$ (SEC) and 44% greater than both short- and long-term exposure to ambient $p\text{CO}_2$ conditions (7 days and 30 days; SAC and LAC) (Fig. 3c; $F_{1,48} = 21.119$, $P = 0.0002$). Very little change in iodine efflux was observed in the untreated control group (Fig. 3c; $F_{1,18} = 107.3027$, $P < 0.0001$). This is supported by significant interactions between $p\text{CO}_2$ and time (Fig. 3c; $F_{1,12.08} = 5.812$, $P = 0.0268$) and $p\text{CO}_2$ and treatment (GG and untreated) (Fig. 3c; $F_{1,28.99} = 5.812$, $P = 0.0268$).

Effect of increasing $p\text{CO}_2$ on iodine accumulation of seaweeds using *in situ* mesocosm experiments

In the mesocosm experiment, elevated $p\text{CO}_2$ increased tissue growth (relative changes in fresh weight) of all three kelp species compared to ambient $p\text{CO}_2$ (Fig. 4 a, b and c, *top panels*; $F_{1, 828} = 332.087$, $P < 0.0001$). This effect was consistent over time, which is supported by a significant interaction between time and $p\text{CO}_2$ conditions (Fig. 4 a, b and c, *top panels*; $F_{1, 828} = 175.387$, $P < 0.0001$). Changes in relative weight were significantly different between the three species (Fig. 4 a, b and c, *top panels*; $F_{2, 828} =$

504.273, $P < 0.0001$), including significant interactions between the species of seaweeds and time (Fig. 4 a, b and c, *top panels*; $F_{2,828} = 38.434$, $P < 0.0001$), and significant interactions between $p\text{CO}_2$ conditions, time and species of seaweeds (Fig. 4 a, b and c, *top panels*; $F_{2,828} = 28.354$, $P < 0.0001$). *M. pyrifera* showed the largest increase in weight under elevated $p\text{CO}_2$ at day 40, compared with *S. japonica* at day 90 and *U. pinnatifida* at day 60. *S. japonica* and *U. pinnatifida* showed similar changes in weight under ambient and elevated $p\text{CO}_2$ until day 30, thereafter *U. pinnatifida* showed larger increases in weight than *S. japonica* by day 60 (Fig. 4a).

Iodine accumulation increased in the three seaweeds under elevated $p\text{CO}_2$ compared to ambient $p\text{CO}_2$ (Fig. 4 a, b and c, *bottom panels*; $F_{1,353} = 36.362$, $P < 0.0001$). The highest iodine accumulation was observed at time zero, thereafter relative iodine accumulation declined with time (Fig. 4 a, b and c, *bottom panels*; $F_{1,353} = 791.782$, $P < 0.0001$) however, iodine accumulation declined more quickly under ambient $p\text{CO}_2$ conditions compared to elevated $p\text{CO}_2$. The three seaweeds species responded with different intensities to changes in $p\text{CO}_2$ (Fig. 4 a, b and c, *bottom panels*; $F_{2,353} = 16.322$, $P < 0.0001$). *S. japonica* showed the highest iodine accumulation at time zero, both under ambient $p\text{CO}_2$ ($7.91 \text{ mg g}^{-1} \text{ dw} \pm 0.13 \text{ SE}$) and elevated $p\text{CO}_2$ ($7.87 \text{ mg g}^{-1} \text{ dw} \pm 0.19 \text{ SE}$), but it also had the greatest decline in iodine accumulation over 90 days (total decline of 85% and 73% for ambient and elevated $p\text{CO}_2$ respectively). Compared to *S. japonica*, *U. pinnatifida* and *M. pyrifera* showed modest iodine accumulation at time zero. Iodine accumulation declined under both ambient and elevated $p\text{CO}_2$ by 58% and

26% respectively, over 60 days in *U. pinnatifida* (Fig. 4b) and 63% and 56%, over 40 days in *M. pyrifera* (Fig. 4c). This variation in iodine accumulation over time is supported by a significant interaction between species of seaweeds and time (Fig. 4 a, b and c, *bottom panels*; $F_{2,353} = 16.553$, $P < 0.0001$). In addition to kelp species (Fig. S6), we also found similar responses to elevated $p\text{CO}_2$ in other seaweeds species, where both algal biomass and iodine accumulation increased with the elevated $p\text{CO}_2$ (Fig. S7).

Iodine transfer between *S. japonica* and its consumer *H. discus* in a mesocosm experiment

In the feeding experiment, abalone fed with *S. japonica*, cultured under elevated $p\text{CO}_2$ (1000 μatm) had a higher iodine accumulation than those fed on seaweeds cultured under ambient $p\text{CO}_2$ (400 μatm) (Fig. 5a, $F_{1,106} = 155.24$, $P < 0.0001$). In addition, iodine accumulation in the abalone was stimulated when the feeding experiments were conducted under elevated $p\text{CO}_2$ (1000 μatm) (Fig. 5a, $F_{1,106} = 29.53$, $P < 0.0001$). Iodine accumulation in all experimental abalone increased over the 30 days of cultivation (Fig. 5a, $F_{1,105} = 1003.48$, $P < 0.0001$), and abalone fed with seaweeds grown under high $p\text{CO}_2$ and under elevated $p\text{CO}_2$ conditions showed the highest amount of iodine accumulation (Fig. 5a; *interaction between diet, time and $p\text{CO}_2$* , $F_{1,102} = 26.29$, $P < 0.0001$). There was no difference in iodine accumulation between feeding experiments conducted in a cage or in the field with no cage (Fig. 5a, $F_{1,103} = 1.31$, $P = 0.255$).

It was found that both T3 (Fig. 5b; $F_{1,33} = 831.98$, $P < 0.0001$) and T4 (Fig. 5b; $F_{1,33} =$

482.77, $P < 0.0001$) hormone concentrations declined when the abalone were fed with *S. japonica* cultured under elevated $p\text{CO}_2$, regardless of the $p\text{CO}_2$ conditions of the feeding experiment. Whilst there was a decline in thyroid concentration under elevated $p\text{CO}_2$, for both T3 (Fig. 5b; $F_{1,34} = 143.29$, $P < 0.0001$) and T4 concentrations ($F_{1,34} = 183.36$, $P < 0.0001$), the largest drop in thyroid concentration occurred when abalone were fed with algae cultured under high $p\text{CO}_2$ and under elevated $p\text{CO}_2$ conditions. Linear regression analysis further demonstrated that dietary inclusion of *S. japonica* with higher iodine content caused an increase in iodine intake into the abalone (Fig. S8a) and resulted in lower concentration of T3 (Fig. S8b) and T4 (Fig. S8c) hormones. Moreover, results also revealed that there were significant negative relationships between iodine concentration and T3 (Fig. S9a) and T4 content (Fig. S9b). Overall, THs concentrations were higher in the field with no cage for both T3 (Fig. 5b; $F_{1,32} = 324.30$, $P < 0.0001$) and T4 (Fig. 5b; $F_{1,32} = 284.49$, $P < 0.0001$) hormones. However, THs concentration drop in field conditions when abalone were fed with algae cultured under elevated $p\text{CO}_2$, and this is supported by a significant interaction between the $p\text{CO}_2$ level that dietary seaweeds were cultured under and the conditions of the feeding experiment (i.e. caged or not caged), for both T3 concentrations (Fig. 5b; $F_{1,31} = 23.93$, $P < 0.0001$) and T4 concentrations (Fig. 5b; $F_{1,31} = 47.16$, $P < 0.0001$).

***In situ* transcriptional or proteomic response of *S. japonica* to elevated $p\text{CO}_2$**

Transcriptome data showed that 11 *vIPO* (vanadium-dependent iodoperoxidases) and 12 *vBPO* (vanadium-dependent bromoperoxidases) UniGenes were significantly

differentially expressed between ambient and elevated $p\text{CO}_2$ of culture environments (Fig. 6a). Among these genes, 8 *vIPOs* and 8 *vBPOs* were down-regulated, whereas 3 *vIPOs* and 4 *vBPOs* were up-regulated under elevated $p\text{CO}_2$ in the mesocosms (Table S2, S3). The variation trend was verified for 8 genes by RT-PCR (Fig. S10). In the proteomic data, it was found that four vHPOs proteins were down-regulated at elevated $p\text{CO}_2$ (Fig. 6b). Therein, the trend of relative expression of two vBPOs (SJ19768 and SJ19850) was consistent with those in the transcriptome. In contrast, vIPOs (SJ00628) and vBPOs (SJ10798) did not significantly change at the transcriptomic level.

DISCUSSION

Brown algae are predicted to benefit from elevated $p\text{CO}_2$ under global change (Enochs et al., 2015; Johnson, Russell, Fabricius, Brownlee, & Hall-Spencer, 2012; Linares et al., 2015; Porzio, Buia, & Hall-Spencer, 2011; Xu et al., 2017) and therefore will thrive in natural $p\text{CO}_2$ rich environments (Enochs et al., 2015; Johnson, Russell, Fabricius, Brownlee, & Hall-Spencer, 2012; Linares et al., 2015; Porzio, Buia, & Hall-Spencer, 2011). It is supported by data that tissue growth of *S. japonica* (Fig. 2 and Fig. 4a), *U. pinnatifida* (Fig. 4b), and *M. pyrifera* (Fig. 4c), and photosynthesis of *S. japonica* (Fig. S11) all increased under elevated CO_2 conditions. However, it was unknown how enhanced growth of kelp, under conditions of ocean acidification, affect the accumulation and transfer of iodine across coastal marine foodwebs. Increasing $p\text{CO}_2$ will not change the solubility and availability of inorganic iodine in seawater (Fig. S5). However, the data presented here reveal for the first time that increasing $p\text{CO}_2$ causes

iodine accumulation in coastal seaweeds and leads to the accumulation of iodine in consumers of kelp, which potentially will result in elevated iodine intake of consumers of kelp if $p\text{CO}_2$ continues to rise (1,000 μatm in 2100 under RCP 8.5) as predicted by climate models (Fig. 1).

In laboratory experiment, we found that at $p\text{CO}_2$ greater than 400 μatm (the current $p\text{CO}_2$ value), changes in temperature had no effect on iodine accumulation and predictions of iodine accumulation in *S. japonica* could be made based on changes in $p\text{CO}_2$ alone (Fig. 2). It is suggested that this is because $p\text{CO}_2$ is the dominant environmental driver when $p\text{CO}_2$ and temperature change simultaneously. This finding is supported by Brennan and Collins (2015) who demonstrated that changes in the growth rate of the microalgae *Chlamydomonas reinhardtii* could be predicted using the dominant environmental driver in test environments with up to eight environmental drivers (Brennan & Collins, 2015). Global change will involve many simultaneous environmental changes, such as changes in CO_2 , pH, temperature, and nutrient (Boyd, Lennartz, Glover, & Doney, 2015; Gruber, 2011; Hutchins & Fu, 2017). Results presented here highlight the importance of measuring the response to multiple environmental drivers in order to understand how they interact. Predictions on the combined effects of environmental drivers using traditional additive or multiplicative models could potentially overestimate the effects of ocean warming and ocean acidification on iodine accumulation (Fig. S12).

Elevated iodine accumulation in *S. japonica* under ocean acidification was associated with down-expression regulation of vHPOs (vIPOs and vBPOs), which has never been observed before in any alga (Fig. 6). While vHPOs specific physiological role is still unclear, these genes have previously been studied for their role in the oxidative stress response in brown algae including, *S. japonica* (Ye et al., 2015) and *Laminaria digitata* (Cosse et al., 2009). In addition, the physiological antioxidant role of iodine in algae is suggested to be linked to the presence of particular vHPOs (Colin et al., 2003, 2005). Under oxidative stress, induced by elicitor-triggered oxidative burst, iodine efflux increased in *S. japonica*, even under high $p\text{CO}_2$ (Fig. 3), supporting the physiological role of iodine in algae. In some cases, the iodine efflux was up to twice as high as in the control group (Fig. 3a). Thus, iodine efflux is probably an efficient strategy to cope with oxidative stress (Küpper et al., 2008). Furthermore, the oligoalginate-triggered oxidative burst and associated iodide release is also known to be an efficient strategy against infection, suggesting that under ocean acidification kelp may be able to cope better with infections as they have more stored iodine (Küpper et al., 2008; Küpper, Müller, Peters, Kloareg, & Potin, 2002).

Elevated iodine content in kelp has the potential to be transferred to their consumers such as abalone. *H. discus* fed with algae cultured under elevated CO_2 showed higher levels of iodine accumulations and reduced levels of T3 and T4 hormones compared to animals fed with algae cultured under ambient CO_2 (Fig. 5). Iodine is essential for the synthesis of thyroid hormones (THs), which play important roles in development,

metamorphosis and metabolism of vertebrates and invertebrates, including humans (Bath et al., 2017; Huang et al., 2015). Previous studies have demonstrated that sea urchin larvae could potentially receive TH precursors or the active hormones from some of the microalgal species that they consumed (Heyland & Moroz, 2006). Whilst, few data were available on the effect of iodine intake on the THs of invertebrates, some studies on humans demonstrate that high-dose kelp supplementation significantly decreased the total triiodothyronine levels of subjects (Eliason, 1998). The increased iodine transfer and reduced thyroid hormones could potentially impact nutrient composition of coastal primary producers as well as in kelp-based coastal food webs.

Our results suggest that projected $p\text{CO}_2$ (1,000 μatm in 2100 under RCP 8.5) will increase the growth of coastal seaweeds and their iodine accumulation, with the potential for higher levels of iodine to be transferred from seaweeds to consumers. Thus, there is a potential risk of iodine overconsumption in consumers of kelps if $p\text{CO}_2$ increases as projected for the coming decades. Furthermore, biogeochemical cycling of iodine in coastal ecosystems might change as a consequence of enhanced accumulation in coastal marine foodwebs. This may even have consequences for coastal non-marine habitats as volatile iodinated compounds can be released to the atmosphere (Cosse, Potin, & Leblanc, 2009; Küpper & Kroneck, 2014).

ACKNOWLEDGEMENTS

We thank F. Weinberger and P. Kroth for revision of the manuscript. This work was

supported by National Natural Science Foundation of China (41676145); Shandong
key Research and Development Plan (2018GHY115010); Central Public-interest
Scientific Institution Basal Research Fund CAFS (2017HY-YJ01); Qingdao
Municipal Science and Technology plan project (17-1-1-96-jch); Special Scientific
Research Funds for Central Non-Profit Institutes, Yellow Sea Fisheries Research
Institute, Chinese Academy of Fishery Sciences (20603022016010,
20603022016001); China Agriculture Research System (CARS-50); Taishan Scholars
Funding; AoShan Talents Program (No. 2015ASTPES03); the Science Fund for
Distinguished Young Scholars of Shandong Province (JQ201509).

REFERENCES

- Bath, S. C., Hill, S., Infante, H. G., Elghul, S., Neziyanya, C. J., & Rayman, M. P. (2017).
Iodine concentration of milk-alternative drinks available in the UK in comparison
with cows' milk. *British Journal of Nutrition*, *118*, 525–532.
- Berg, V., Nøst, T. H., Skeie, G., Thomassen, Y., Berlinger, B., Veyhe, A. S., ... Hansen,
S. (2017). Thyroid homeostasis in mother–child pairs in relation to maternal iodine
status: the MISA study. *European Journal of Clinical Nutrition*, *71*, 1002–1007.
- Bloom, A. J., Burger, M., Asensio, J. S. R., & Cousins, A. B. (2010). Carbon dioxide
enrichment inhibits nitrate assimilation in wheat and *Arabidopsis*. *Science*, *328*,
899–903.
- Boyd, P. W., Lennartz, S. T., Glover, D. M., & Doney, S. C. (2015). Biological
ramifications of climate-change-mediated oceanic multi-stressors. *Nature Climate*

529 *Change*, 5, 71.

530 Brennan, G., & Collins, S. (2015). Growth responses of a green alga to multiple
531 environmental drivers. *Nature Climate Change*, 5, 892.

532 Butler, A., & Carter-Franklin, J. N. (2004). The role of vanadium bromoperoxidase in
533 the biosynthesis of halogenated marine natural products. *Natural Product Reports*,
534 21, 180–188.

535 Colin, C., Leblanc, C., Michel, G., Wagner, E., Leize-Wagner, E., Van Dorsselaer, A.,
536 & Potin, P. (2005). Vanadium-dependent iodoperoxidases in *Laminaria digitata*, a
537 novel biochemical function diverging from brown algal bromoperoxidases. *JBIC*
538 *Journal of Biological Inorganic Chemistry*, 10, 156–166.

539 Colin, C., Leblanc, C., Wagner, E., Delage, L., Leize-Wagner, E., Van Dorsselaer, A., ...
540 & Potin, P. (2003). The brown algal kelp *Laminaria digitata* features distinct
541 bromoperoxidase and iodoperoxidase activities. *Journal of Biological Chemistry*,
542 278, 23545.

543 Cosse, A., Potin, P., & Leblanc, C. (2009). Patterns of gene expression induced by
544 oligoguluronates reveal conserved and environment-specific molecular defense
545 responses in the brown alga *Laminaria digitata*. *New Phytologist*, 182, 239–250.

546 Dillon, M. E., Wang, G., & Huey, R. B. (2010). Global metabolic impacts of recent
547 climate warming. *Nature*, 467, 704.

548 Eliason, B. C. (1998). Transient hyperthyroidism in a patient taking dietary
549 supplements containing kelp. *The Journal of the American Board of Family*
550 *Practice*, 11, 478–480.

551 Enochs, I. C., Manzello, D. P., Donham, E. M., Kolodziej, G., Okano, R., Johnston,
552 L., ... & Valentino, L. (2015). Shift from coral to macroalgae dominance on a
553 volcanically acidified reef. *Nature Climate Change*, 5, 1083.

554 Gruber, N. (2011). Warming up, turning sour, losing breath: ocean biogeochemistry
555 under global change. *Philosophical Transactions of the Royal Society of London*
556 *A: Mathematical, Physical and Engineering Sciences*, 369, 1980–1996.

557 Guillard, R. R. L. (1975). Culture of phytoplankton for feeding marine invertebrates.
558 In W. L. Smith & M. H. Chanley (Eds.), *Culture of marine invertebrate animals*
559 (pp. 26–60). New York, NY: Plenum Press.

560 Heyland, A., & Moroz, L. L. (2006). Signaling mechanisms underlying metamorphic
561 transitions in animals. *Integrative and Comparative Biology*, 46, 743–759.

562 Huang, W., Xu, F., Qu, T., Zhang, R., Li, L., Que, H., & Zhang, G. (2015). Identification
563 of thyroid hormones and functional characterization of thyroid hormone receptor
564 in the pacific oyster *Crassostrea gigas* provide insight into evolution of the thyroid
565 hormone system. *PloS One*, 10, e0144991.

566 Hutchins, D. A., & Fu, F. (2017). Microorganisms and ocean global change. *Nature*
567 *Microbiology*, 2, 17058.

568 Jin, P., Wang, T., Liu, N., Dupont, S., Beardall, J., Boyd, P. W., ... & Gao, K. (2015).
569 Ocean acidification increases the accumulation of toxic phenolic compounds
570 across trophic levels. *Nature Communications*, 6, 8714.

571 Johnson, V. R., Russell, B. D., Fabricius, K. E., Brownlee, C., & Hall-Spencer, J. M.
572 (2012). Temperate and tropical brown macroalgae thrive, despite decalcification,

573 along natural CO₂ gradients. *Global Change Biology*, 18, 2792–2803.

574 Küpper, F. C. (2015). Iodine in Seaweeds—Two Centuries of Research. In Springer
575 Handbook of Marine Biotechnology (pp. 591–596). Springer, Berlin, Heidelberg.

576 Küpper, F. C., & Kroneck, P. M. (2014). Iodine bioinorganic chemistry: physiology,
577 structures, and mechanisms. *Iodine Chemistry and Applications*, 555–589.

578 Küpper, F. C., Carpenter, L. J., McFiggans, G. B., Palmer, C. J., Waite, T. J., Boneberg,
579 E. M., ... & Potin, P. (2008). Iodide accumulation provides kelp with an inorganic
580 antioxidant impacting atmospheric chemistry. *Proceedings of the National*
581 *Academy of Sciences*, 105, 6954–6958.

582 Küpper, F. C., Kloareg, B., Guern, J., & Potin, P. (2001). Oligoguluronates elicit an
583 oxidative burst in the brown algal kelp *Laminaria digitata*. *Plant Physiology*, 125,
584 278–291.

585 Küpper, F. C., Müller, D. G., Peters, A. F., Kloareg, B., & Potin, P. (2002). Oligoalginate
586 recognition and oxidative burst play a key role in natural and induced resistance
587 of sporophytes of Laminariales. *Journal of Chemical Ecology*, 28, 2057–2081.

588 Leung, A. M., & Braverman, L. E. (2014). Consequences of excess iodine. *Nature*
589 *Reviews Endocrinology*, 10, 136.

590 Linares, C., Vidal, M., Canals, M., Kersting, D. K., Amblas, D., Aspillaga, E., ... &
591 Hereu, B. (2015). Persistent natural acidification drives major distribution shifts
592 in marine benthic ecosystems. *Proc. R. Soc. B*, 282, 20150587.

593 Loladze, I. (2002). Rising atmospheric CO₂ and human nutrition: toward globally
594 imbalanced plant stoichiometry?. *Trends in Ecology & Evolution*, 17, 457–461.

595 Martínez-Botí, M. A., Foster, G. L., Chalk, T. B., Rohling, E. J., Sexton, P. F., Lunt, D.
 596 J., ... & Schmidt, D. N. (2015). Plio-Pleistocene climate sensitivity evaluated using
 597 high-resolution CO₂ records. *Nature*, 518, 49.

598 McKibben, S. M., Peterson, W., Wood, A. M., Trainer, V. L., Hunter, M., & White, A.
 599 E. (2017). Climatic regulation of the neurotoxin domoic acid. *Proceedings of the*
 600 *National Academy of Sciences*, 114, 239–244.

601 Myers, S. S., Smith, M. R., Guth, S., Golden, C. D., Vaitla, B., Mueller, N. D., ... &
 602 Huybers, P. (2017). Climate change and global food systems: potential impacts on
 603 food security and undernutrition. *Annual Review of Public Health*, 38, 259–277.

604 Nitschke, U., & Stengel, D. B. (2015). A new HPLC method for the detection of iodine
 605 applied to natural samples of edible seaweeds and commercial seaweed food
 606 products. *Food Chemistry*, 172, 326–334.

607 Phalkey, R. K., Aranda-Jan, C., Marx, S., Höfle, B., & Sauerborn, R. (2015). Systematic
 608 review of current efforts to quantify the impacts of climate change on
 609 undernutrition. *Proceedings of the National Academy of Sciences*, 112, 4522–4529.

610 Pierrot, D. E., Lewis, E., & Wallace, D. W. R. (2006). MS Excel program developed for
 611 CO₂ system calculations. Oak Ridge, TN: Carbon Dioxide Information Analysis
 612 Center, Oak Ridge National Laboratory, U.S. Department of Energy. doi:
 613 10.3334/CDIAC/otg.CO2SYS_XLS_CDIAC105a

614 Porzio, L., Buia, M. C., & Hall-Spencer, J. M. (2011). Effects of ocean acidification on
 615 macroalgal communities. *Journal of Experimental Marine Biology and Ecology*,
 616 400, 278–287.

617 R Core Development Team. (2014). R: A language and environment for statistical
618 computing: R Foundation for Statistical Computing. <http://www.R-project.org/>.

619 Strittmatter, M., Grenville-Briggs, L. J., Breithut, L., Van West, P., Gachon, C. M., &
620 Küpper, F. C. (2016). Infection of the brown alga *Ectocarpus siliculosus* by the
621 oomycete *Eurychasma dicksonii* induces oxidative stress and halogen metabolism.
622 *Plant Cell & Environment*, 39, 259–271.

623 Sunday, J. M., Fabricius, K. E., Kroeker, K. J., Anderson, K. M., Brown, N. E., Barry,
624 J. P., ... & Klinger, T. (2017). Ocean acidification can mediate biodiversity shifts
625 by changing biogenic habitat. *Nature Climate Change*, 7, 81.

626 Thomsen, J., Stapp, L. S., Haynert, K., Schade, H., Danelli, M., Lannig, G., ... &
627 Melzner, F. (2017). Naturally acidified habitat selects for ocean acidification–
628 tolerant mussels. *Science Advances*, 3, e1602411.

629 Ullah, H., Nagelkerken, I., Goldenberg, S. U., & Fordham, D. A. (2018). Climate
630 change could drive marine food web collapse through altered trophic flows and
631 cyanobacterial proliferation. *PLoS Biology*, 16, e2003446.

632 Xu, D., Schaum, C. E., Lin, F., Sun, K., Munroe, J. R., Zhang, X. W., ... & Ye, N. (2017).
633 Acclimation of bloom-forming and perennial seaweeds to elevated $p\text{CO}_2$
634 conserved across levels of environmental complexity. *Global Change Biology*, 23,
635 4828–4839.

636 Ye, N., Zhang, X., Miao, M., Fan, X., Zheng, Y., Xu, D., ... & Wang, Y. (2015).
637 *Saccharina* genomes provide novel insight into kelp biology. *Nature*
638 *Communications*, 6, 6986.

Zhang, K., Song, C., Zhang, Y., Dang, H., Cheng, X., & Zhang, Q. (2018). Global-scale patterns of nutrient density and partitioning in forests in relation to climate. *Global Change Biology*, 24, 536–551.

Zhu, C., Kobayashi, K., Loladze, I., Zhu, J., Jiang, Q., Xu, X., ... & Fukagawa, N. K. (2018). Carbon dioxide (CO₂) levels this century will alter the protein, micronutrients, and vitamin content of rice grains with potential health consequences for the poorest rice-dependent countries. *Science Advances*, 4, eaaq1012.

SUPPORTING INFORMATION

Additional Supporting Information may be found in the online version of this article:

Table S1. Carbonate system data (mean ± standard errors) in the laboratory set up using the CO2SYS Package.

Table S2. The genes used for real-time quantitative PCR (RT-qPCR) *S. japonica* cultured in field experiment under ambient (bubbled with air) and elevated *p*CO₂ (bubbled with mix air of 1,000 µatm CO₂).

Table S3. The primers used for real-time quantitative PCR (RT-qPCR) of *S. japonica* cultured in field experiment under ambient (bubbled with air) and elevated *p*CO₂ (bubbled with mix air of 1,000 µatm CO₂).

Fig. S1. Kinetics of iodine influx by *S. japonica* sporophyte under of various concentrations of KI. (a) Iodine influx rate (IIR) of *S. japonica* sporophyte. (b) The Lineweaver-Burk plots between KI substrate and iodine influx rate which was used for

Lineweaver-Burk K_m and IUR_{max} determination. In a laboratory set up, kinetics of iodine influx of *S. japonica* under a series of iodide concentration in surrounding medium were determined over a duration of 24 hours. With increasing concentration of iodide (1-30 $\mu\text{mol L}^{-1}$ KI), the influx rate increased significantly until the external KI concentration exceeded 10 $\mu\text{mol L}^{-1}$ (One-Way ANOVA, $df=5$, $P<0.001$). Furthermore, iodine influx followed a Michaelis-Menten equation and Lineweaver-Burk plot was used for $K_{1/2}$ (19.94 $\mu\text{mol L}^{-1}$) and IIR_{max} (15.04 $\mu\text{mol g}^{-1}$ dry weight h^{-1}) determination ($R^2=0.9547$, $df=1$, $F=84.229$, $P<0.05$).

Fig. S2. Experimental design of the field experiment. $p\text{CO}_2$ treatments were carried out in triplicate tanks ($n=3$ per $p\text{CO}_2$ level), under ambient $p\text{CO}_2$ (400 μatm , bubbled with air) and elevated $p\text{CO}_2$ (bubbled with air/ CO_2 premixed gas using a CO_2 Enrichlor). In the field experiment, we held all seaweed species simultaneously as logistics did not allow for each species to be grown on its own at each $p\text{CO}_2$ level at sufficient replication. The letters in the net cages represent experimental algal species used in the mesocosms including *S. japonica* (a), *U. pinnatifida* (b), *M. pyrifera* (c), *G. lemaneifor* (d), *G. chouae* (e), *U. pertusa* (f), and *U. intestinalis* (g).

Fig. S3. Example for coastal mesocosms on the sea. (a) photograph of net cages and CO_2 Enrichlor used for ocean acidification experiment; (b) Variation of nutrient (mean \pm standard errors, $n=6$); (c) Variation in temperature; (d) Variation of irradiance. During the culture period (160 days), the seawater temperature initially decreased from 10.36 ± 0.44 $^{\circ}\text{C}$ to 2.08 ± 0.17 $^{\circ}\text{C}$ after 80 days and then increased from 2.37 ± 0.48 $^{\circ}\text{C}$ to 12.73 ± 0.22 $^{\circ}\text{C}$. The average irradiance was 98 $\mu\text{mol photons m}^{-2} \text{ s}^{-1}$ and the light

condition would not limit algal growth.

Fig. S4. Variation of seawater carbonate chemistry (mean \pm standard error) under low (400 μ atm bubbled with air) or high $p\text{CO}_2$ (1,000 μ atm bubbled with air/ CO_2 premixed gas using a CO_2 Enrichlor) conditions for more than 5 months in the coastal field experiment. (a) pH; (b) Total alkalinity (TA); (c) DIC; (d) HCO_3^- ; (e) CO_3^{2-} ; (f) CO_2 . The shaded areas indicate the standard deviation of three replicates.

Fig. S5. The individual and combined effect of increasing $p\text{CO}_2$ and temperature on iodine solubility and availability. Colored columns show the observed variation of iodide (a) or iodate (b) concentration of three biological replicates (\pm SE) under increasing $p\text{CO}_2$ at different temperatures of 5°C, 10°C, 15°C, 20°C and 25°C.

Fig. S6. Algal fresh weight (top panels) and iodine accumulation (bottom panels) under ambient $p\text{CO}_2$ (400 μ atm, bubbled with air, blue) and elevated $p\text{CO}_2$ (bubbled with mix air of 1,000 μ atm CO_2 , red) for (a) *S. japonica*, (b) *U. pinnatifida*, and (c) *M. pyrifera* in mesocosm experiments. Colored circles show the average of biological replicates at each time point (\pm SE), with $n=30$ for fresh weight and $n=18$ for iodine accumulation.

Fig. S7. Algal fresh weight (top panels) and iodine accumulation (bottom panels) under ambient $p\text{CO}_2$ (400 μ atm, bubbled with air, blue) and elevated $p\text{CO}_2$ (bubbled with mix air of 1,000 μ atm CO_2 , red) for (a) *U. pertusa*, (b) *U. intestinalis*, (c) *G. lemaneiformis*, and (d) *G. chouae* in mesocosm experiment. Colored circles show the average of biological replicates at each time (\pm SE), with $n=30$ for fresh weight and $n=18$ for iodine accumulation.

Fig. S8. Linear regression analysis between the iodine concentration of *S. japonica* and iodine concentration or THs synthesis in the consumer *H. discus*. (a) Linear regression analysis between the iodine concentration in *S. japonica* and iodine concentration in *H. discus*; (b) Linear regression analysis between the iodine concentration in *S. japonica* and T3 concentration in *H. discus*; (c) Linear regression analysis between the iodine concentration in *S. japonica* and T4 concentration in *H. discus*.

Fig. S9. Linear regression analysis between the iodine concentration and THs synthesis in *H. discus*. (a) Linear regression analysis between the iodine concentration and T3 concentration; (b) Linear regression analysis between the iodine concentration and T4 concentration.

Fig. S10. Relative expression level of several *vHPO* genes by real-time quantitative PCR (RT-qPCR).

Fig. S11. The individual and combined effects of temperature and $p\text{CO}_2$ on F_v/F_m of *S. japonica* in laboratory set up. (a) The individual effect of increasing temperature on F_v/F_m where culture $p\text{CO}_2$ was set at 400 μatm and bubbled with air; (b) The individual effect of increasing $p\text{CO}_2$ on F_v/F_m where the temperature was maintained at 10 °C; (c) The combined effects of high temperature of 15 °C and increasing $p\text{CO}_2$ on F_v/F_m ; (d) The combined effects of high temperature of 20 °C and increasing $p\text{CO}_2$ on F_v/F_m .

Fig. S12. Comparing the observed effect and the predicted effect of increasing $p\text{CO}_2$ and temperature on the kelp *S. japonica*. Filled circles show the

observed response in total iodine accumulation of three biological replicates (\pm SE) under increasing $p\text{CO}_2$ at different temperatures; 10°C (grey), 15°C (yellow) and 20°C (blue). Colored solid lines show the predicted response of iodine accumulation under increasing $p\text{CO}_2$ at different temperatures; 15°C (yellow) and 20°C (blue) using (a) the additive model and (b) the multiplicative model. The dashed grey line shows the observed response of increasing $p\text{CO}_2$ under control temperature conditions (10°C). This is equivalent to predictions based on the dominant environmental driver (in this example the dominant driver is $p\text{CO}_2$) and demonstrates that predictions on iodine accumulation in *S. japonica* are most accurate when based on the response to $p\text{CO}_2$ alone. Note that the y-axis differ between panels a and b.

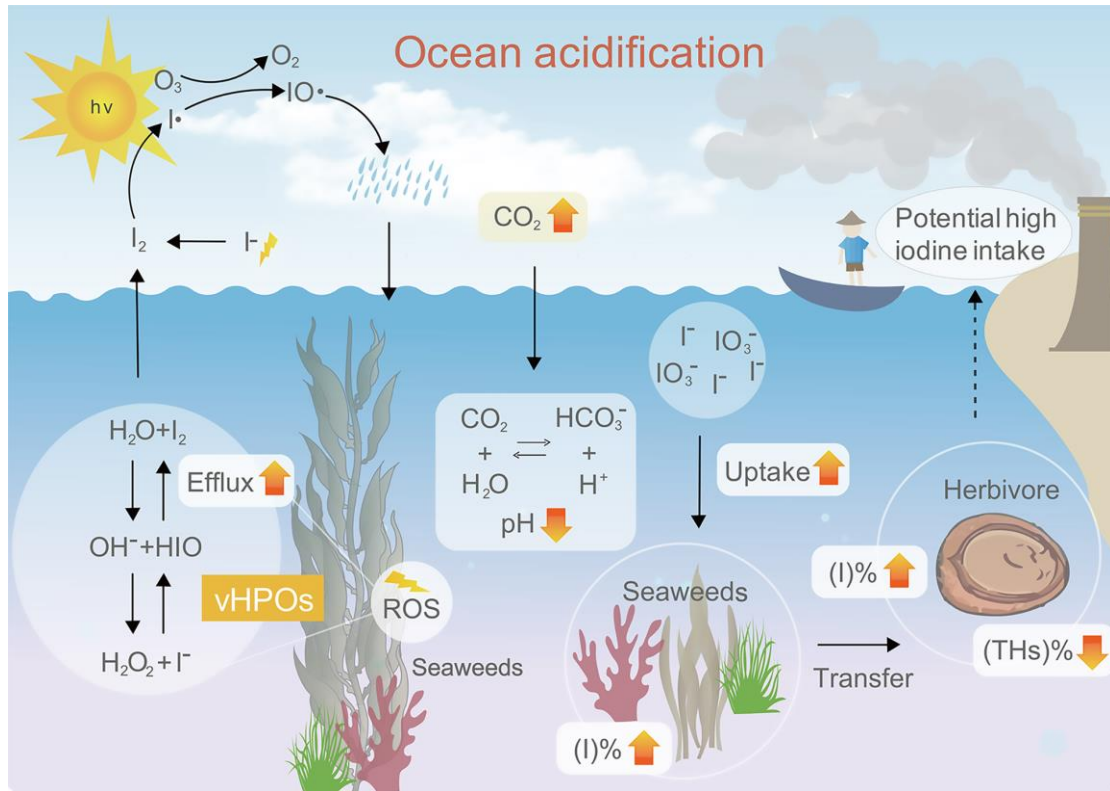


Fig. 1. Conceptual diagram showing altered iodine metabolic pathway and global iodine geochemical cycle under ocean acidification. The yellow up arrows indicate the up-regulated pathway; the yellow down arrows indicate the down-regulated pathway; the black arrow with dashed lines indicates the possible outcome under further ocean acidification. The abbreviations ROS represents the reactive oxygen species; vHPOs represents the vanadium-dependent haloperoxidases; THs represents the thyroid hormones.

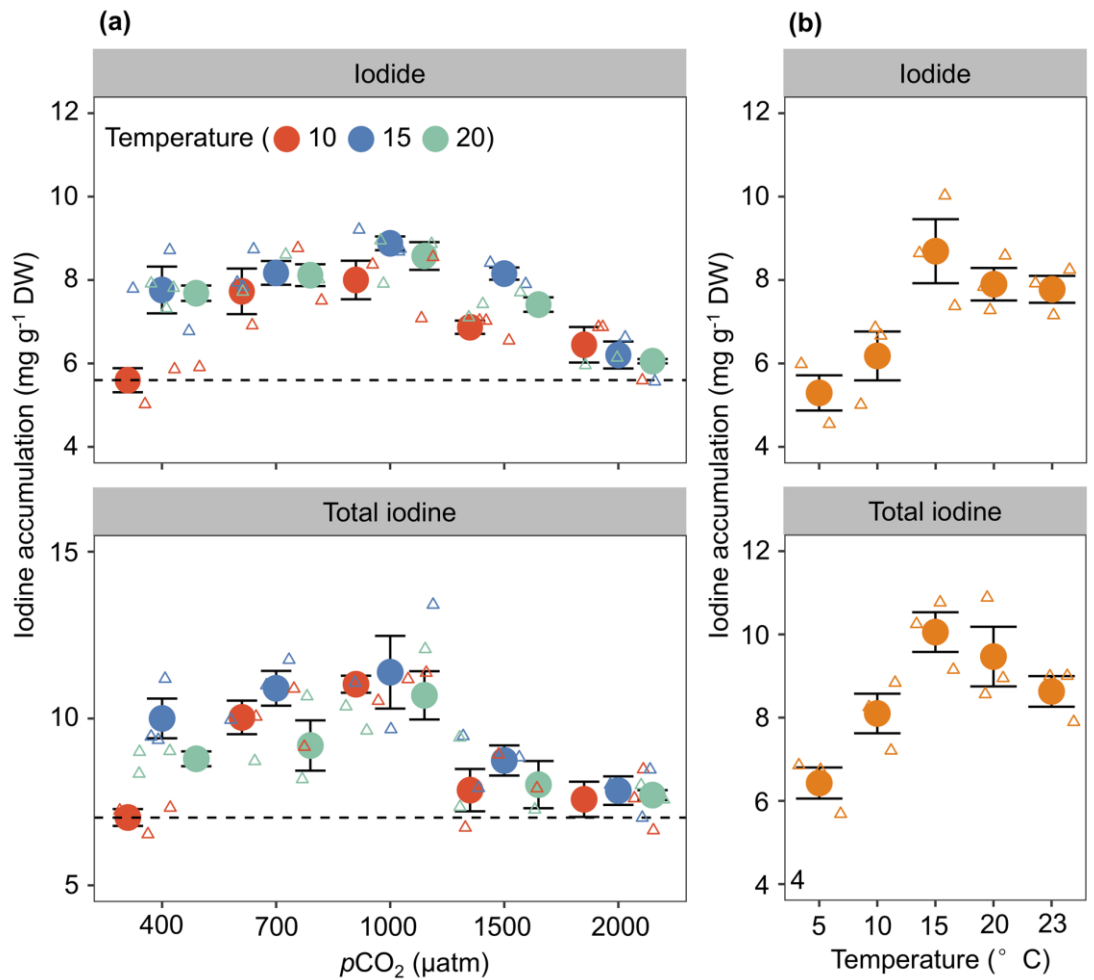


Fig. 2. The combined effect of increasing $p\text{CO}_2$ and temperature and the effect of increasing temperature alone on iodine accumulation in the kelp *S. japonica*. Filled circles show the average iodide (top panels) and total iodine (bottom panels) accumulation in three biological replicates (\pm SE). (a) Colored circles show the combined effects of increasing $p\text{CO}_2$ at different temperatures; 10°C (red), 15°C (blue) and 20°C (green). Horizontal dashed lines indicate the iodine accumulation under control temperature (10°C) and $p\text{CO}_2$ (400 μatm) conditions. (b) Colored circles (orange) show that iodide and total iodine accumulation increases with increasing temperature under control $p\text{CO}_2$ levels (400 μatm).

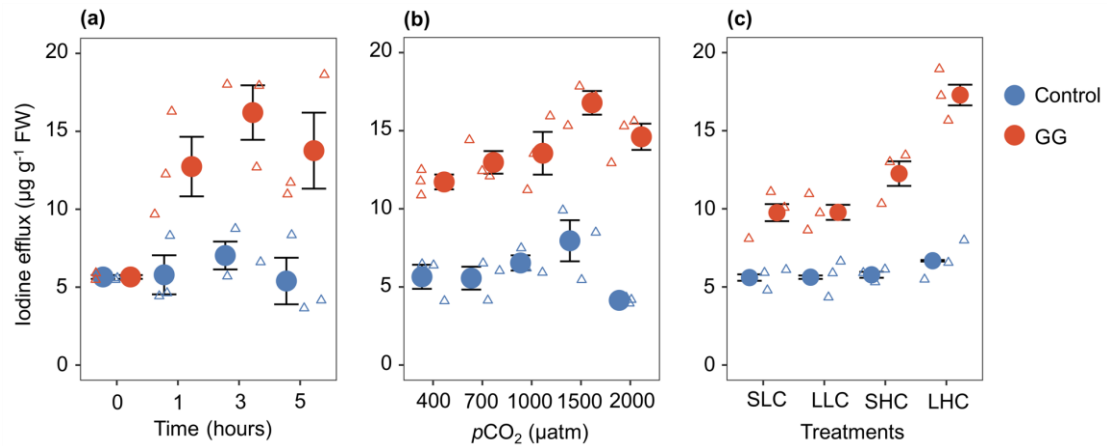


Fig. 3. The effect of increasing $p\text{CO}_2$ on iodine efflux of *S. japonica* upon oligogulonate-triggered oxidative burst in laboratory experiment. Colored circles show the average iodine efflux of three biological replicates (\pm SE) under oligogulonate elicitor (GG, blue) and Control (red) conditions. (a) The change in iodine efflux of *S. japonica* under GG and control conditions over 5 hours at 10°C ; (b) The effect of increasing $p\text{CO}_2$ on iodine efflux of *S. japonica* after 3 hours of GG elicitation at 10°C ; (c) The short-term elevated $p\text{CO}_2$ vs long-term elevated $p\text{CO}_2$ effect on iodine efflux 10°C . Treatments shown in the x-axis denote the culture conditions of *S. japonica*; SAC = short-term (7 days) under ambient carbon (400 μatm), SEC = short-term (7 days) under elevated-carbon (1,000 μatm), LAC = long-term (30 days) under ambient-carbon (400 μatm), and LEC = long-term (30 days) under elevated-carbon (1,000 μatm).

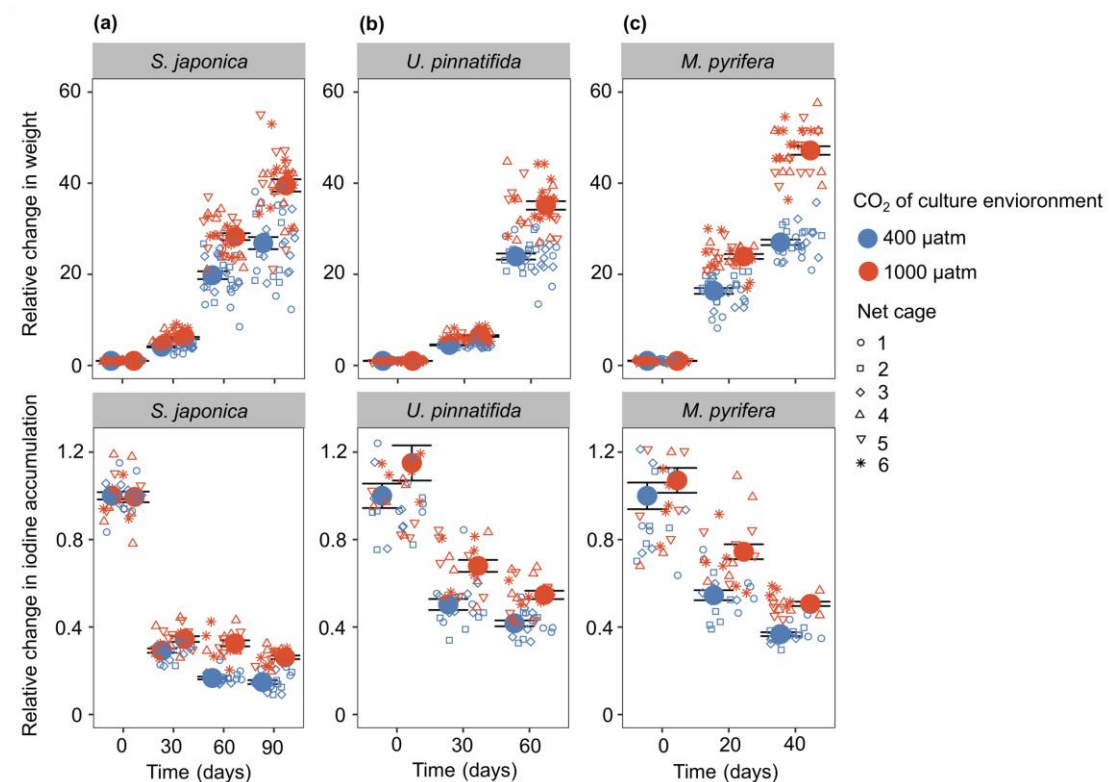


Fig. 4. Relative changes in weight (top panels) and relative changes in iodine accumulation (bottom panels) under ambient $p\text{CO}_2$ (400 μatm , bubbled with air, blue) and elevated $p\text{CO}_2$ (bubbled with mix air of 1,000 μatm CO₂, red), in a mesocosm experiment. Three kelp species (a) *S. japonica*, (b) *U. pinnatifida*, (c) *M. pyrifera* were cultured in mesocosm experiment. Colored circles show the average of biological replicates at each time (\pm SE), with $n=30$ for the relative changes in weight and $n=18$ for the relative changes in iodine.

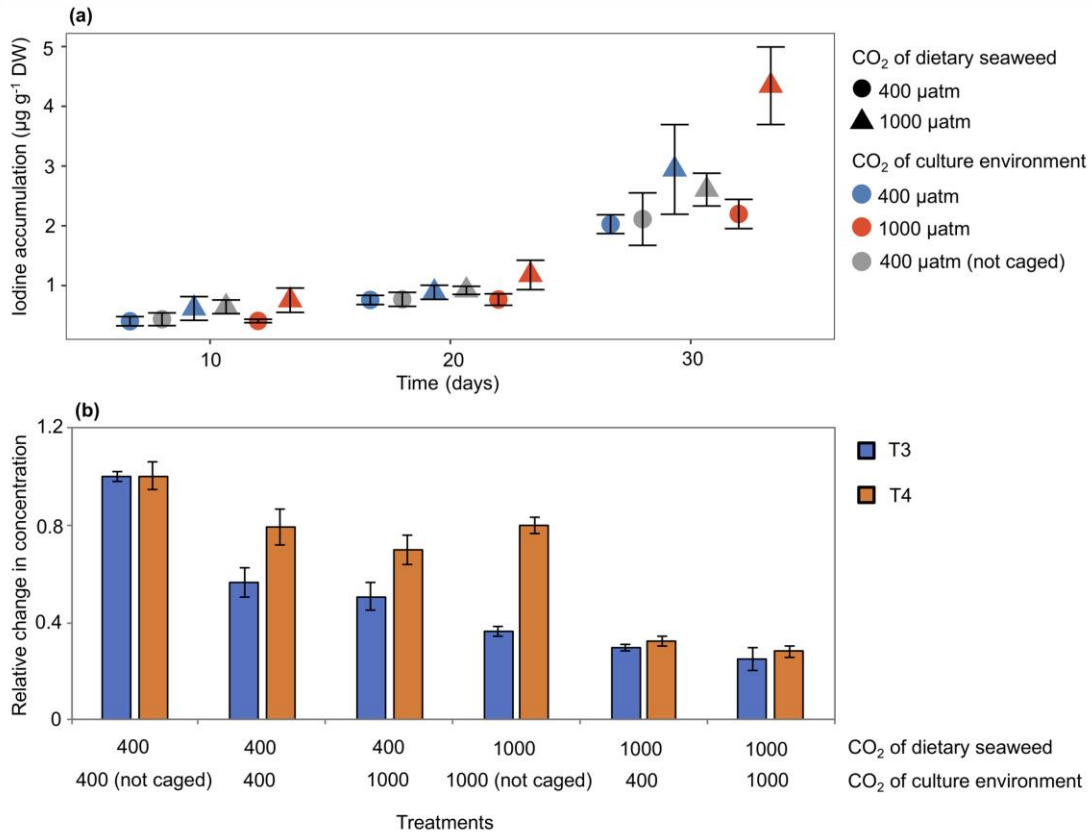


Fig. 5. Changes in iodine accumulation and thyroid hormones (THs) synthesis in *H. discus* fed with seaweeds cultured under either ambient and elevated $p\text{CO}_2$. Colored symbols show the average iodine accumulation of six biological replicates (\pm SE) fed with either *S. japonica* cultured under 400 μatm (circles) or 1,000 μatm (triangles) $p\text{CO}_2$. Feeding trials were conducted inside a cage under either 1,000 μatm (red symbols) or 400 μatm (blue symbols) $p\text{CO}_2$ or in the field with no cage under 400 μatm (gray symbols) $p\text{CO}_2$. (a) Changes in iodine accumulation in *H. discus* were measured every 10 days for 30 days. (b) Changes in the concentrations of triiodothyronine (T3) and thyroxine (T4) at day 30, relative to data collected from feeding experiments with algae cultured under 400 μatm , in the field.

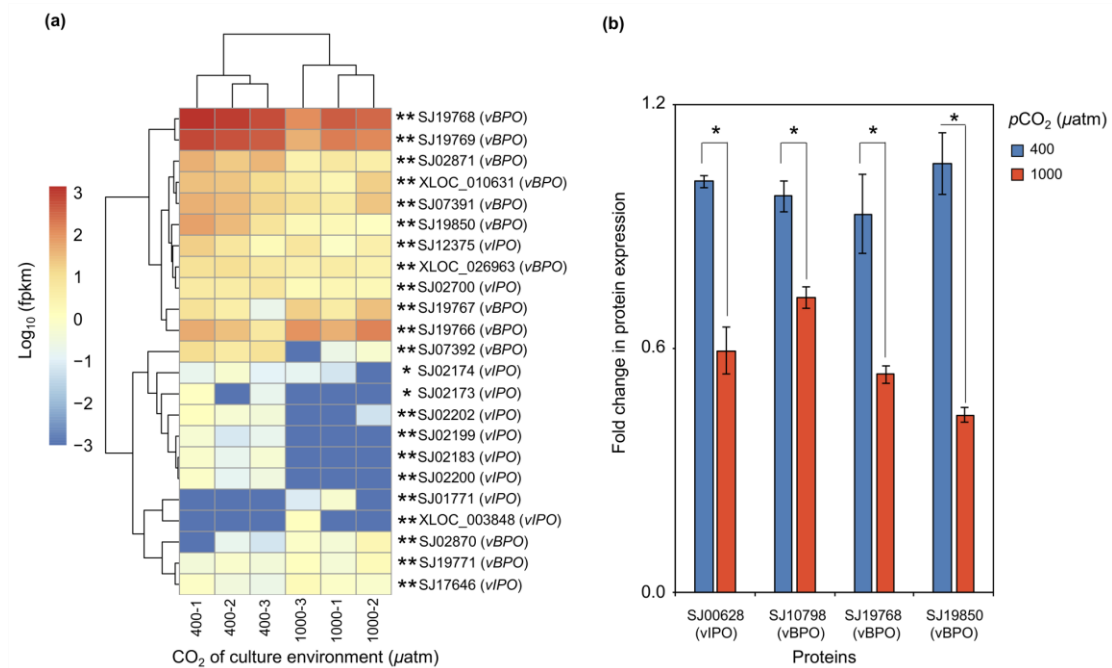


Fig. 6. The effect of increasing $p\text{CO}_2$ on the relative expression of vHPO at transcriptomic or proteomic level in *S. japonica* cultured under ambient (400 μatm) or elevated (1,000 μatm) $p\text{CO}_2$ scenarios, using an *in situ* mesocosm experiment.

(a) Variation of vHPO gene expression; (b) Variation of vHPO protein expression. * (p-value <0.05) and ** (p-value <0.001) represent significant differences between treatments of ambient (400 μatm) or high (1,000 μatm) $p\text{CO}_2$.